Available online at www.sciencedirect.com
ScienceDirect
Applied Catalysis B: Environmental 80 (2008) 195–201
APPLIED CATALYSIS B: ENVIRONMENTAL
www.elsevier.com/locate/apcatb

Hydrogen effect on the preferential oxidation of carbon monoxide over alumina-supported gold nanoparticles

Elodie Quinet [a], Franck Morfin [a], Fabrice Diehl [b], Priscilla Avenier [b], Valérie Caps [a,*], Jean-Luc Rousset [a]

[a] *Institut de recherches sur la catalyse et l'environnement de Lyon (IRCELYON, CNRS-University of Lyon), 2 avenue Albert Einstein, F-69626 Villeurbanne Cedex, France*
[b] *IFP-Lyon, Direction Catalyse & Séparation, BP 3, F-69390 Vernaison, France*

Received 27 September 2007; received in revised form 13 November 2007; accepted 17 November 2007
Available online 22 November 2007

Abstract

Although alumina-supported gold nanoparticles are poor catalysts for the oxidation of carbon monoxide, they have turned out to be promising candidates for the preferential oxidation of CO in hydrogen-rich streams (PrOx), as hydrogen apparently enhances the CO oxidation rate. The mechanism of this promotion effect is unclear. In this study, we carry out kinetic measurements on the PrOx reaction catalyzed by a 0.9% Au/Al_2O_3 catalyst, which is prepared by direct anionic exchange. We show that the apparent activation energy of the oxidation of CO is lower than that of the oxidation of H_2, whatever the hydrogen content in the feed. On the other hand, the hydrogen partial reaction order is higher in the oxidation of H_2 than in the oxidation of CO. Thus, the CO oxidation rate is significantly increased at low temperature by the introduction of only a small amount of hydrogen in the reactant mixture. At higher temperatures, the selectivity to CO_2 decreases due to competition with the oxidation of H_2. Higher hydrogen concentrations cause the competition between CO and H_2 oxidations to start at lower temperatures. It is proposed that hydrogen reacts with oxygen to yield highly oxidizing intermediates that selectively react with CO as long as the energetic barrier to produce water from these intermediates is not crossed.

Keywords: Hydrogen; Gold; Alumina; PrOx; CO oxidation; $H_2 + O_2$ intermediates

1. Introduction

The preferential oxidation of CO in the presence of hydrogen (PrOx: $CO + (1/2)O_2 + H_2 \rightarrow CO_2 + H_2$) is a reaction of interest for the purification of the gas feeding proton-exchange membrane fuel cells (PEM-FC). CO is indeed an unavoidable by-product of hydrogen production from steam reforming of hydrocarbon fuels, that needs to be removed from the stream. Otherwise, it will poison the platinum-based electrode that converts hydrogen to electricity, thereby decreasing the overall efficiency of the fuel cell. The key-challenge is to achieve high conversion of CO at low temperature (near the operating temperature of the PEM-FC: 80–120 °C) without oxidizing the hydrogen fuel.

Gold catalysts have turned out to be more active at low temperature than platinum-based catalysts for the oxidation of pure carbon monoxide [1]. Nevertheless, supported gold nanoparticles display variable catalytic performances depending on the support. A clear evidence of this can be found in two studies [2,3], in which the effect of the support is isolated from other parameters known to influence the catalytic activity of supported gold nanoparticles, such as the metal particle size [4]. CO oxidation rate was observed to be higher on Au/TiO_2 than on Au/ZrO_2, Au/ZnO and Au/Al_2O_3. One reason would be the enhancement on the most reducible oxides of the oxygen activation, which cannot take place on the gold particle [5]. The oxygen vacancies of the transition metal oxide supports indeed provide additional sites for oxygen activation and reaction with the interface hydroxycarbonyl species, proposed as intermediate in the oxidation of CO [6,7]. For pure CO oxidation, gold supported on non-reducible alumina was found to be very poor catalyst, as no ‘‘active’’ oxygen is available on this material.

* Corresponding author. Tel.: +33 472 445 331; fax: +33 472 445 399.
E-mail address: valerie.caps@ircelyon.univ-lyon1.fr (V. Caps).

0926-3373/$ – see front matter © 2007 Elsevier B.V. All rights reserved.
doi:10.1016/j.apcatb.2007.11.011

However, in the presence of hydrogen, CO conversion is significantly enhanced on Au/Al_2O_3, slightly enhanced on Au/ZrO_2 while it remains essentially unchanged over Au/TiO_2 [8], which makes this alumina catalyst industrially attractive for the PEM-FC technology. A better understanding of the hydrogen promotion effect on the CO oxidation rate is however required before optimization of the gold–alumina system can be undertaken. In particular, the mechanism of oxygen activation in the presence of hydrogen on the non-reducible Au/Al_2O_3 system seems to be crucial.

Several authors have shown that the presence of hydrogen in CO/O_2 mixtures allows to reduce and even prevent deactivation of many gold catalysts, such as Au/MnO_x [9], Au/FeO_x [10,11], Au/TiO_2 [12] or Au/Al_2O_3 [13–15] operating at low temperature. On Au/TiO_2 [16] and Au/Al_2O_3 [17], it has been proposed that hydrogen (or water formed from its reaction with oxygen) inhibits the formation of formate and carbonate species (formed from reaction of CO with the surface hydroxycarbonyl species) which are thought to be poisons for the oxidation of CO. The presence of hydrogen in the reaction mixture can also reduce these poison species to regenerate the catalyst [18]. Some authors have directly observed a promotion effect of hydrogen on Au/Al_2O_3-catalyzed CO oxidation [19,20], which was related to the higher adsorption rate and lower desorption rate of CO on Au/Al_2O_3 observed in the presence of H_2 [21]. We recently proposed [8,22] that hydroperoxy-type species are formed from the reaction of hydrogen with oxygen over gold [23], that are more reactive than molecular oxygen towards CO, as it is proposed for the Au/TiO_2-catalyzed gas phase epoxidation of propylene [24–27].

In this paper, we focus on the understanding of the key-role of hydrogen in the low temperature PrOx reaction over Au/Al_2O_3. We present a kinetic study that has been carried out over a γ-Al_2O_3-supported gold catalyst in the range 20–280 °C. We propose a mechanism for the oxidation of CO in the presence of hydrogen over Al_2O_3-supported gold nanoparticles, based on our experimental data and on a theoretical model from the recent literature.

2. Experimental

2.1. Catalyst preparation

Before the synthesis, the support (pellets of γ-Al_2O_3 with a BET surface area of 140 $m^2\ g^{-1}$ manufactured by AXENS) was crushed and sieved in order to obtain a powder with a grain size in the range 125–210 μm. Then the alumina-supported gold catalyst was synthesized by a direct anionic exchange method [28]. A 1.42×10^{-4} mol L^{-1} $HAuCl_4$ (Alfa-Aesar, 99.99%) aqueous solution was prepared and added to the support (1 g). The solution was heated to 70 °C and stirred for 1 h. The slurry was filtered and washed with warm water. The catalyst was re-suspended in an ammonia solution for 1 h in order to minimize the amount of the remaining chlorine on the surface and washed with water again. After the final filtration, the catalyst was dried in an oven at 120 °C overnight and calcined in air at 300 °C for 4 h using a heating rate of 5 °C min^{-1}.

2.2. Catalyst characterization

2.2.1. Chemical analysis

The gold loading was determined by using inductively coupled plasma atom emission spectroscopy (ICP-AES). The chlorine loading was determined by ionic chromatography at the CNRS Center for Chemical Analysis (Vernaison, France).

2.2.2. Morphology and size distribution of gold particles

Transmission electron microscopy (TEM) observations were performed on a JEOL 2010 microscope equipped with an Oxford EDX spectrometer and operated at 200 kV. To obtain suitable samples for TEM characterization the powder was dispersed in ethanol by ultrasonication. A drop of the solution was then deposited onto a thin holey carbon film supported on a copper microscopy grid and left to dry. The mean particle diameters were calculated from size distributions determined by measuring over 200 particles.

2.2.3. Surface analysis

X-ray photoelectron spectroscopy (XPS) surface analyses were recorded with a Kratos Axis Ultra DLD spectrometer using a hemispherical analyzer and working in ultra-high vacuum ($P < 10^{-9}$ mbar). The data were acquired using monochromated Al Kα radiation (1486.6 eV, 150 W), a pass energy of 40 eV and a hybrid lens mode. The analyzed surface area is 700 μm × 300 μm. Charge neutralization was required for the sample. The binding energy scale was corrected for surface charging by taking the C 1s peak of contaminant carbon as a reference at 284.6 eV.

2.3. Catalytic studies

Two kinds of studies were performed. On the one hand, the catalytic performances of the catalyst were evaluated through three reactions: CO oxidation, H_2 oxidation and preferential CO oxidation in H_2-rich stream in order to estimate the influence of each gas on the conversion of the others. On the other hand, a kinetic study on the influence of hydrogen on CO oxidation was carried out by varying the amount of hydrogen in the reactant gas mixture.

Activity measurements were carried out in a continuous flow fixed bed reactor at atmospheric pressure and variable temperature. 27 mg of gold catalyst diluted in γ-Al_2O_3 (in order to obtain a catalytic bed height of 14 mm/800 mg) were introduced in the quartz tube reactor located in a ceramic furnace. The reactant gases were mixed with mass flow controllers (Brooks Instrument) and sent through the reactor at a total flow rate of 50 mL min^{-1} corresponding to a gas hourly space velocity (GHSV) of ∼2100 h^{-1}. The gas mixtures consisted in 2% CO, 2% O_2 for CO oxidation, 48% H_2, 2% O_2 for H_2 oxidation, 2% CO, 48% H_2, 2% O_2 for preferential CO oxidation in H_2 stream and 2% CO, 4% O_2, x% H_2 (x = 0.25 to 75) for the kinetic study, all balanced in helium. The reaction was temperature programmed between ambient and 280 °C with a heating rate of 1 °C min^{-1}, using a thermocouple located inside the catalytic bed to control the furnace heating power. A

second thermocouple placed also within the catalytic bed allows to acquire the reaction temperature that is used to draw the light-off curves. Several reaction cycles, each consisting of a heating and a cooling period, were recorded to monitor possible hysteresis behavior, deactivation or activation. The outlet gases were analyzed with an online VARIAN-Micro GC (CP2003) equipped with a TCD detector. Two columns were used in parallel: a Molsieve 5Å column (Ar as carrier gas) to quantify H_2, O_2 and CO and a poraPLOT Q column (He as carrier gas) to quantify CO_2.

Mass-specific CO or H_2 oxidation rates (mol g_{Au}^{-1} s^{-1}) were determined for the concentration of each component at the in- and out-lets of the reactor:

$$r_{CO} = \frac{y_{CO,in} \times X_{CO} \times V_{gas}}{m_{Au}} \quad \text{or} \quad r_{H_2} = \frac{y_{H_2,in} \times X_{H_2} \times V_{gas}}{m_{Au}}$$

m_{Au} is the mass of Au in the catalytic bed in g; V_{gas} the total molar flow rate in mol s^{-1}; X_{CO} (X_{H_2}) the conversion of CO (conversion of H_2); $y_{CO,in}$ ($y_{H_2,in}$) is the mole fraction of CO (H_2) in the in-let gas mixture.

Selectivity to CO_2 at a given temperature in the PrOx reaction is defined as $r_{CO}/(r_{CO} + r_{H_2})$.

3. Results and discussion

3.1. Catalyst characterization

The physico-chemical properties of the Au/γ-Al_2O_3 material are given in Table 1. The 140 m^2 g^{-1} alumina catalyst contains 0.92 wt.% of gold, which is close to the intended 1% gold loading. The chlorine content is below 10 ppm, illustrating the efficiency and the interest of the ammonia wash during the catalyst synthesis. The average particle size of gold is 5.8 nm with a standard deviation of 2.2 nm as determined from the particle size distribution presented in Fig. 1. The binding energy of the Au $4f_{7/2}$ core level is found at 83.1 eV, which is lower than the value for bulk gold Au^0 (84.0 eV). This indicates that gold particles are slightly negatively charged, which has already been observed for other Au/Al_2O_3 materials [2]. As this exceeds the extent of the surface-core level shift expected from small particle size, it is attributed to a charge transfer from the alumina support to the gold particle. No evidence of the presence of cationic gold [29] is detected.

3.2. Catalytic results

The catalytic properties of this material in CO oxidation, H_2 oxidation and PrOx reaction under standard conditions (2% CO/2% O_2/48% H_2) are shown in Fig. 2. For clarity, only data

Table 1
Physico-chemical properties of the alumina-supported nanoparticles

Catalyst	Au/γ-Al_2O_3
Au loading (wt.%)	0.92
Surface area (m^2 g^{-1})	140
Au mean particle diameter (nm) TEM	5.8
Oxidation state of gold (XPS)	$Au^{\delta-}$ (Au $4f_{7/2}$ 83.1 eV)

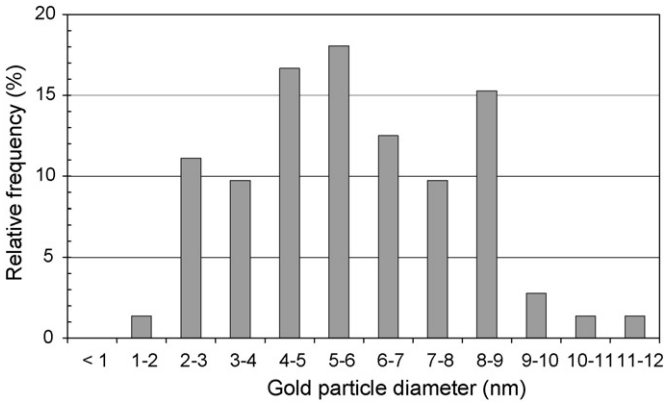

Fig. 1. Particle size distribution of gold dispersed on γ-alumina via the direct anionic exchange method.

corresponding to the first cooling step are plotted and will be used for discussion in what follows. Data obtained on the second step are similar, indicating that the catalyst is stable under the reaction conditions used.

The oxidation of hydrogen is only slightly inhibited by the presence of CO: the H_2 oxidation light-off temperature is not affected but at higher temperatures (>105 °C), H_2 conversion does not reach its maximum values. On the other hand, and as generally observed on Au/Al_2O_3 catalysts [8], the CO oxidation rate is substantially enhanced at low temperature by the presence of hydrogen. CO conversion at 100 °C increases from few percents to nearly 65% and the maximum conversion in PrOx is nearly doubled by comparison with pure CO oxidation. At higher temperatures, the drop in the CO conversion in PrOx is due to both competition between H_2 and CO oxidation and the lack of oxygen in the feed. To overcome or at least delay this issue, the following kinetic study has been carried out with 4% O_2 in the feed, which is the maximum oxygen fraction allowed to remain within a non-explosive range of O_2/H_2 + CO mixture.

The effects of hydrogen on the oxidation rates of CO and H_2 have been further studied by varying the H_2 concentration in the PrOx reaction. Kinetic data (activation energies, reaction rates

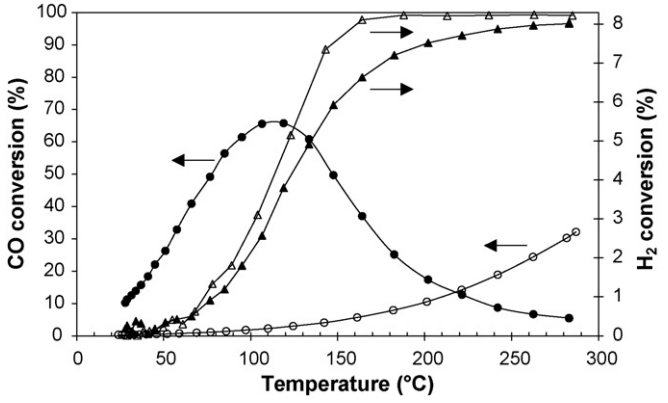

Fig. 2. CO and H_2 conversions as functions of temperature for the Au/γ-Al_2O_3 catalyzed oxidation of CO in the presence (●) and in the absence of hydrogen (○) and for the Au/γ-Al_2O_3 catalyzed oxidation of H_2 in the presence (▲) and in the absence of CO (△). Reaction conditions: (2% CO), 2% O_2, (48% H_2) balanced in helium.

Table 2
Catalytic properties of Au/γ-Al_2O_3 in the PrOx reaction using various concentrations of hydrogen

$y_{H_2,in}$[a], %	E_a (kJ mol^{-1}), 4% O_2[b]		E_a (kJ mol^{-1}), 2% O_2[c]			T (°C)[d]	Reaction rates[e] (mmol g_{Au}^{-1} s^{-1})		Sel.[f] (100 °C), %
	COprox	H_2prox	COprox	H_2prox	H_2ox	$r_{COprox} \cap r_{H_2prox}$	COprox	H_2prox	
0	–	–	26	–	–	–	0.021	–	–
0.25	31 ± 3	36 ± 3	–	–	–	≫280	0.156	0.032	95
0.5	27 ± 3	43 ± 3	–	–	–	≫280	0.174	0.050	93
1	34 ± 3	46 ± 3	–	–	–	>280	0.225	0.100	89
5	26 ± 3	32 ± 3	–	–	–	215	0.276	0.128	87
10	30 ± 3	45 ± 3	–	–	–	180	0.279	0.142	86
20	22 ± 3	44 ± 3	–	–	–	150	0.332	0.372	75
48	38 ± 3	60 ± 3	34	38	55	110	0.623	1.128	61
75	28 ± 3	48 ± 3	–	–	–	120	0.665	0.940	66

[a] Mole fraction of hydrogen in the PrOx reaction mixture.
[b] Apparent activation energies for the oxidations of CO (COprox) and H_2 (H_2prox) in the PrOx reaction, as calculated from Fig. 3.
[c] Apparent activation energies for the oxidations of CO and H_2 in the presence or in the absence of the other reactant, as calculated from Fig. 2.
[d] Temperature at which the rate for H_2 oxidation (r_{H_2prox}) becomes higher than that for CO oxidation (r_{COprox}) in the PrOx reaction.
[e] Reaction rates given at 50 °C for COprox and at 100 °C for H_2prox.
[f] Selectivity to CO_2 in the PrOx reaction at 100 °C.

and selectivity) are given in Table 2. Oxidation rates of CO and H_2 as a function of temperature and H_2 molar fraction are reported in Fig. 3a and b, respectively. Again, only data corresponding to the first cooling step are plotted and used for discussion. Subsequent steps are identical, showing that the catalyst is stable whatever the concentration of hydrogen in the feed.

At low temperature, the rate of the Au/Al_2O_3-catalyzed CO oxidation is strongly enhanced by the introduction of even a very small amount of hydrogen (0.25%) in the reactant mixture. Both CO and H_2 oxidation rates increase with increasing hydrogen concentration. Fig. 3 furthermore shows that the low temperature promotion effect of H_2 on CO oxidation is effective from room temperature, far below the temperature at which hydrogen starts to be consumed in the formation of water (∼120 °C for $y_{H_2,in} < 10\%$ and ∼70 °C for $y_{H_2,in} > 10\%$). This suggests that a water promotion effect is unlikely [13,20,30,31] and that hydrogen might directly take part in the mechanism of CO oxidation in PrOx.

All CO oxidation rate curves display an inflexion or a maximum point in the range 120–170 °C. For hydrogen fractions up to 10%, CO conversions at the highest temperatures tend to reach those observed in the absence of hydrogen. For hydrogen fractions above 10%, CO conversions collapse, at higher temperatures, because of a lack of available oxygen (Fig. 4a) which is continuously consumed by the competitive oxidation of hydrogen that produces water (Fig. 3b), as commonly observed in the literature [9,13,15,16].

The lower selectivity to CO_2 as the temperature increases (Fig. 4b) is related to an apparent activation energy which is higher for the oxidation of H_2 than for the oxidation of CO in PrOx [10]. Our data confirm that the activation energy for CO oxidation is always lower than that for H_2 oxidation whether in the presence or in the absence of the other reactant (Fig. 5). This remains valid for each concentration of hydrogen used in the PrOx reaction mixture (Fig. 6, Table 2). Moreover, the selectivity to CO_2 (Fig. 4b, Table 2) is found to decrease (from 95% to about 60% at 100 °C) with increasing hydrogen fraction (from 0.25% to 75%) in the reaction mixture, which can be explained by an increase in oxidation rate that is more significant for H_2 than for CO. The H_2 partial reaction order (determined from Fig. 7) is found to be indeed higher for the

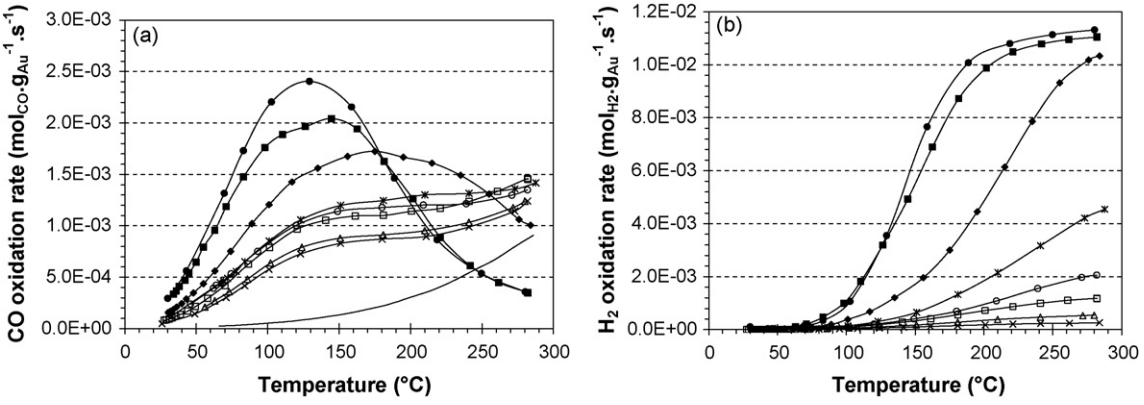

Fig. 3. CO oxidation rate (a) and H_2 oxidation rate (b) vs. temperature in the PrOx reaction over Au/γ-Al_2O_3, using various molar fractions of H_2 in the reactant feed: (×) 0.25%, (△) 0.50%, (□) 1%, (○) 5%, (*) 10%, (◆) 20%, (■) 48%, and (●) 75%. The black curve in (a) is the oxidation of CO in the absence of H_2 (as in Fig. 2) shown for comparison.

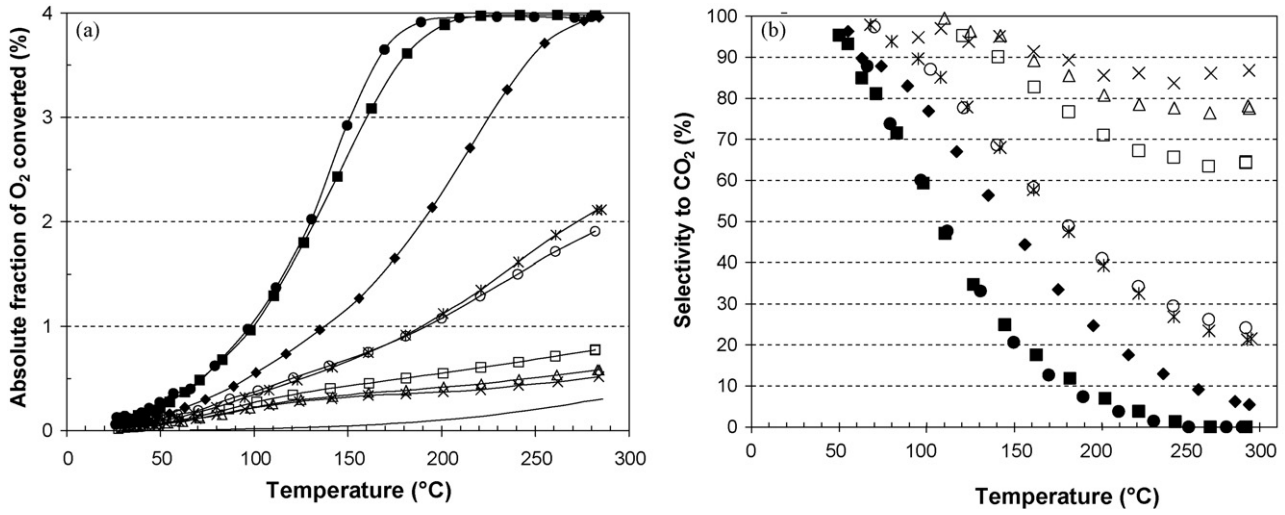

Fig. 4. O_2 conversion (a) and selectivity to CO_2 (b) in the Au/γ-Al_2O_3 catalyzed PrOx reaction (2% CO/4% O_2), using various fractions of H_2 in the reactant feed: (×) 0.25%, (△) 0.50%, (□) 1%, (○) 5%, (*) 10%, (◆) 20%, (■) 48%, and (●) 75%. The black curve in (a) is the conversion of oxygen in the H_2-free oxidation of CO (2% CO/2% O_2), shown for comparison.

oxidation of H_2 ($\alpha_{H_2}^{H_2PrOx} = 0.58$) than for the oxidation of CO ($\alpha_{H_2}^{COPrOx} = 0.24$) under PrOx conditions.

3.3. Proposed mechanism

A recently published kinetic study [32] shows that the direct synthesis of water over silica supported nanoparticles relies on the formation of hydrogen peroxy surface species (–OOH) from reaction between oxygen, that is associatively adsorbed on gold, and dissociatively adsorbed hydrogen. Subsequent reaction between gas phase hydrogen and these –OOH species will produce $–H_2O_2$, –OH and $–H_2O$ surface species, as shown in Scheme 1. The rate-limiting step is proposed to be the formation of $–H_2O_2$ from –OOH, due to its high activation energy (step 2).

This means that, in the presence of both oxygen and hydrogen, highly active –OOH species are formed on the surface of the gold catalyst. Thus, as soon as our catalyst gets in contact with the PrOx mixture ($CO/O_2/H_2$ atmosphere), surface gold atoms become covered with these –OOH species, even before the catalyst is ramped to 280 °C. We propose that, as long as the energetic barrier of the reaction between –OOH and H_2 is not overcome, these species are immediately available to react with CO.

Therefore, at low temperatures (i.e. those at which step (2) cannot proceed), CO would be oxidized using these –OOH surface species and H_2 should be the limiting reactant, the oxidation of CO being directly related to the amount of –OOH formed from H_2 via step (1). The apparent H_2 partial reaction order for the oxidation of CO in PrOx is however quite low ($\alpha_{H_2}^{COPrOx} = 0.24$). This accounts for the fact that the introduction of 0.25% hydrogen in the CO oxidation mixture substantially increases the CO oxidation rate while a drastic increase of the H_2 concentration (to 75%) only further improves the initial CO oxidation rate by 4 times (Table 2). It shows that the lowest fraction of H_2 in the feed is enough to provide a significant ‘‘reservoir’’ of –OOH species on the gold surface. Increasing the hydrogen concentration only slightly changes its capacity. Hydrogen, which is dissociated on gold sites as evidenced experimentally [33], thus activates adsorbed oxygen without being consumed. When oxygen atoms are consumed from –OOH species in the reaction with CO to CO_2, the remaining H*

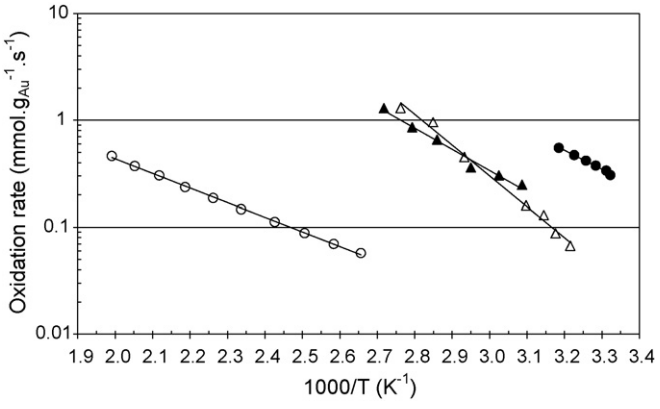

Fig. 5. Determination of activation energies (Table 2) for the Au/γ-Al_2O_3 catalyzed oxidations of CO in the presence (●) and in the absence of hydrogen (○) and for the Au/γ-Al_2O_3 catalyzed oxidations of H_2 in the presence (▲) and in the absence of CO (△). Reaction conditions: (2% CO), 2% O_2, (48% H_2) balanced in helium. Only the points corresponding to a conversion of the minor reactant below 20% are plotted.

$O_2^* + H^* \leftrightarrow OOH^* + *$ step (1)

$OOH^* + H_2 + * \leftrightarrow H_2O_2^* + H^*$ step (2)

$H_2O_2^* + * \leftrightarrow 2OH^*$ step (3)

$OH^* + H^* \leftrightarrow H_2O^* + *$ step (4)

Scheme 1. Mechanism of the gold-catalyzed formation of water from oxygen and hydrogen, as presented in Ref. [32]. The rate-determining step is written in bold characters.

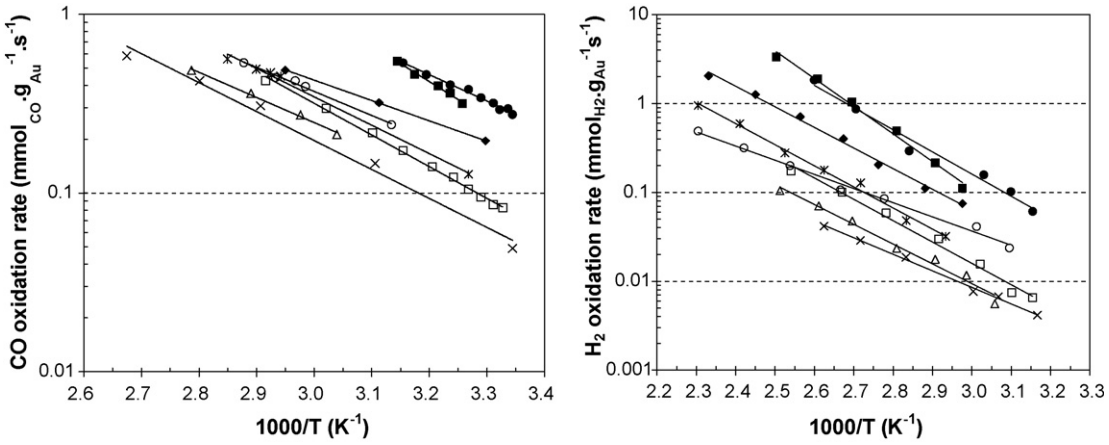

Fig. 6. Determination of activation energies (Table 2) for the Au/γ-Al_2O_3 catalyzed oxidations of CO (a) and H_2 (b) in PrOx mixtures, using various concentrations of H_2 in the reactant feed: (×) 0.25%, (△) 0.50%, (□) 1%, (○) 5%, (*) 10%, (◆) 20%, (■) 48%, and (●) 75%.

might subsequently react with O_2* (Scheme 1, step 1) to form new –OOH species and get CO oxidation running.

When the temperature is reached, at which step (2) can proceed, CO and H_2 will compete for reaction with –OOH species. This light-off temperature for H_2 oxidation significantly depends on the concentration of hydrogen, as the H_2 partial reaction order for the oxidation of hydrogen in PrOx ($\alpha_{H_2}^{H_2PrOx} = 0.58$) is approximately twice that for the oxidation of CO. It basically decreases from 120 °C to 70 °C when hydrogen fraction increases from 0.25% to 75% (Fig. 3b). At that point, the rate for CO oxidation however remains higher than that for H_2 oxidation (Fig. 3), as oxygen is not limiting (less than 20% of available oxygen is consumed; Fig. 4a). The selectivity to CO_2 is therefore high (>85%, Fig. 4b) even in hydrogen-rich streams.

As the temperature further increases, the rate of the oxidation of hydrogen will exceed that of the oxidation of CO. This "threshold" temperature depends on the hydrogen content of the feed. For hydrogen fraction below 1%, the H_2 oxidation rate never exceeds the CO oxidation rate in the temperature range studied (up to 280 °C, Fig. 3, Table 2) and the selectivity to CO_2 remains high (>60%, Fig. 4b). With 5% hydrogen in the feed, H_2 oxidation will be faster than CO oxidation from about 215 °C and this temperature regularly decreases to about 110 °C with increasing H_2 concentration (Table 2). At that point, the selectivity to CO_2 becomes lower than 40% (Fig. 4b), as –OOH species will be preferentially consumed in the reaction with H_2 to form water.

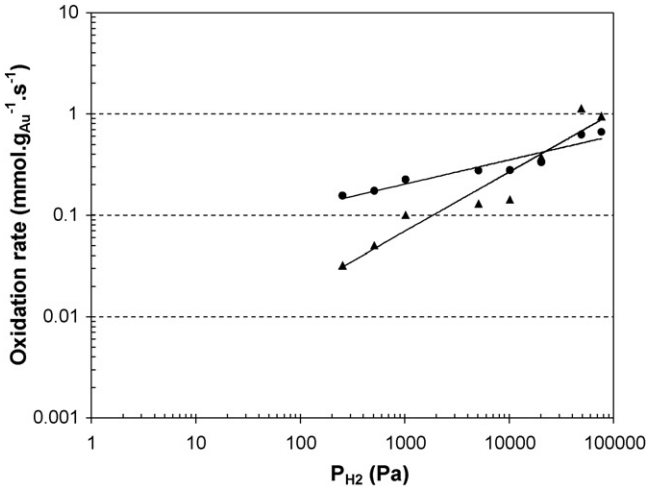

Fig. 7. Determination of the hydrogen partial reaction orders for the oxidation of CO (●) and the oxidation of H_2 (▲) in the PrOx reactions over Au/γ-Al_2O_3 at 50 °C and 100 °C, respectively.

4. Conclusion

We have shown that the positive effect of hydrogen on the low temperature CO oxidation rate in the Au/Al_2O_3-catalyzed PrOx reaction is not a simple water promotion effect. Hydrogen is indeed directly involved in the reaction mechanism of the oxidation of CO, as the CO oxidation rate is enhanced before hydrogen starts to be oxidized. Our kinetic data show that the apparent activation energy for CO oxidation is lower than that for H_2 oxidation in PrOx, whatever the concentration of hydrogen in the feed, resulting in a top selectivity to CO_2 at low temperature, even in hydrogen-rich streams. The hydrogen partial reaction order in PrOx is lower for the oxidation of CO than for the oxidation of H_2. Therefore, even a small hydrogen content in the reactant feed substantially enhances the CO oxidation rate while increasing the hydrogen concentration causes the competition between CO and H_2 for oxygenated species to occur at lower temperatures. On the basis of a study of the oxidation of hydrogen, we propose that hydrogen reacts with associatively adsorbed oxygen to yield highly oxidizing surface intermediates that converts CO to CO_2 at low temperature and that will preferentially react with hydrogen at higher temperatures.

Acknowledgements

The authors wish to acknowledge Dr. D. Uzio for initiating the work, L. Massin for XPS measurements, P. Mascunan and N. Cristin for chemical analyses.

References

[1] M. Haruta, N. Yamada, T. Kobayahsi, S. Iijima, J. Catal. 115 (1989) 301–309.
[2] S. Arrii, F. Morfin, A.J. Renouprez, J.L. Rousset, J. Am. Chem. Soc. 126 (2004) 1199–1205.
[3] M. Comotti, W.-C. Li, B. Spliethoff, F. Schüth, J. Am. Chem. Soc. 128 (2006) 917–924.
[4] M. Haruta, Gold Bull. 37 (2004) 27–36.
[5] M.M. Schubert, S. Hackenberg, A.C. van Veen, M. Muhler, V. Plzak, R.J. Behm, J. Catal. 197 (2001) 113–122.
[6] G.C. Bond, D.T. Thompson, Gold Bull. 33 (2000) 41–51.
[7] C.K. Costello, M.C. Kung, H.S. Oh, Y. Wang, H.H. Kung, Appl. Catal. A 232 (2002) 159–168.
[8] C. Rossignol, S. Arrii, F. Morfin, L. Piccolo, V. Caps, J.-L. Rousset, J. Catal. 230 (2005) 476–483.
[9] R.M.T. Sanchez, A. Ueda, K. Tanaka, M. Haruta, J. Catal. 168 (1997) 125–127.
[10] M.J. Kahlich, H.A. Gasteiger, R.J. Behm, J. Catal. 182 (1999) 430–440.
[11] D.A. Bulushev, L. Kiwi-Minsker, I. Yuranov, E.I. Suvorova, P.A. Buffat, A. Renken, J. Catal. 210 (2002) 149–159.
[12] J.H. Yang, J.D. Henao, M.C. Raphulu, Y. Wang, T. Caputo, A.J. Groszek, M.C. Kung, M.S. Scurrell, J.T. Miller, H.H. Kung, J. Phys. Chem. B 109 (2005) 10319–10326.
[13] R.J.H. Grisel, B.E. Nieuwenhuys, J. Catal. 199 (2001) 48–59.
[14] C.K. Costello, J. Guzman, J.H. Yang, Y.M. Wang, M.C. Kung, B.C. Gates, H.H. Kung, J. Phys. Chem. B 108 (2004) 12529–12536.
[15] S.S. Pansare, A. Sirijaruphan, J.G. Goodwin, J. Catal. 234 (2005) 151–160.
[16] B. Schumacher, Y. Denkwitz, V. Plzak, M. Kinne, R.J. Behm, J. Catal. 224 (2004) 449–462.
[17] C.K. Costello, J.H. Yang, H.Y. Law, Y. Wang, J.N. Lin, L.D. Marks, M.C. Kung, H.H. Kung, Appl. Catal. A 243 (2003) 15–24.
[18] M. Azar, V. Caps, F. Morfin, J.-L. Rousset, A. Piednoir, J.-C. Bertolini, L. Piccolo, J. Catal. 239 (2006) 307–312.
[19] R.J.H. Grisel, C.J. Weststrate, A. Goossens, M.W.J. Craje, A.M. van der Kraan, B.E. Nieuwenhuys, Catal. Today 72 (2002) 123–132.
[20] J.T. Calla, R.J. Davis, Ind. Eng. Chem. Res. 44 (2005) 5403–5410.
[21] D. Gavril, A. Georgaka, V. Loukopoulos, G. Karaiskakis, B.E. Nieuwenhuys, Gold Bull. 39 (2006) 192–199.
[22] M. Lomello-Tafin, A. Ait Chaou, F. Morfin, V. Caps, J.-L. Rousset, Chem. Commun. (2005) 388–390.
[23] M. Okumura, Y. Kitagawa, K. Yamaguchi, T. Akita, S. Tsubota, M. Haruta, Chem. Lett. 32 (2003) 822–823.
[24] T. Hayashi, K. Tanaka, M. Haruta, J. Catal. 178 (1998) 566–575.
[25] T.V. Choudhary, D.W. Goodman, Top. Catal. 21 (2002) 25–34.
[26] T.A. Nijhuis, B.M. Weckhuysen, Catal. Today 117 (2006) 84–89.
[27] A.M. Joshi, W.N. Delgass, K.T. Thomson, J. Phys. Chem. C 111 (2007) 7841–7844.
[28] S. Ivanova, C. Petit, V. Pitchon, Appl. Catal. A 267 (2004) 191–201.
[29] S. Carrettin, J. Guzman, A. Corma, Angew. Chem. Int. Ed. 44 (2005) 2242–2245.
[30] M. Date, M. Haruta, J. Catal. 201 (2001) 221–224.
[31] M. Date, M. Okumura, S. Tsubota, M. Haruta, Angew. Chem. Int. Ed. 43 (2004) 2129–2132.
[32] D.G. Barton, S.G. Podkolzin, J. Phys. Chem. B 109 (2005) 2262–2274.
[33] F. Boccuzzi, A. Chiorino, M. Manzoli, D. Andreeva, T. Tabakovay, J. Catal. 188 (1999) 176–185.